# Supplemental Materials for “Prestressed Vibration of Stiffened Variable Angle Tow Laminated Plates”

Wei Zhao* and Rakesh K. Kapania†

*Virginia Polytechnic Institute and State University, Blacksburg, VA, 24061*

November 11, 2018

## Contents



*Post-doctoral Fellow, Kevin T. Crofton Department of Aerospace and Ocean Engineering, weizhao@vt.edu, AIAA Member

†Norris and Wendy Mitchell Endowed Professor, Kevin T. Crofton Department of Aerospace and Ocean Engineering, rkapania@vt.edu, AIAA Associate Fellow

# 1 Verification Results for Free Vibration of unstiffened VAT laminated plate

## 1.1 Complete free vibration mode shapes (Section III.A)

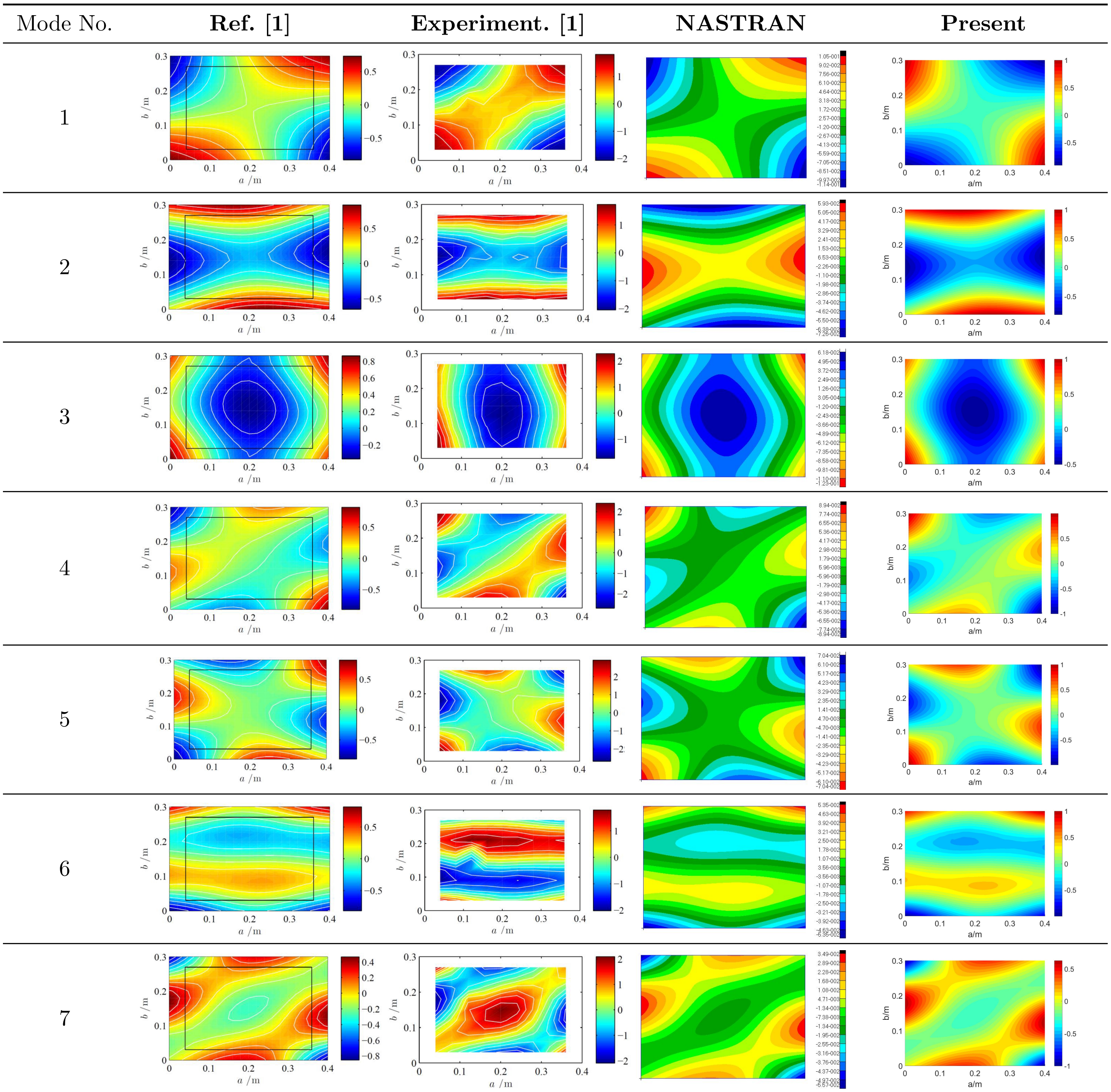


Figure 1: The complete first 7 elastic mode shapes for a free rectangular VAT laminated plate

### 1.2 Free vibration mode frequency values of a clamped square VAT plate (Section III.B)

Table 1: Comparisons of cycle frequency for a fully clamped square VAT laminated plate (unit: rad/s), the value shown in the bracket () is obtained from FEM (Ref. [2])

| Mode No. | $[\pm\langle 45\vert -45\rangle]_{2,\mathrm{S}}$ | $[\pm\langle 45\vert -30\rangle]_{2,\mathrm{S}}$ | $[\pm\langle 45\vert -15\rangle]_{2,\mathrm{S}}$ | $[\pm\langle 45\vert 0\rangle]_{2,\mathrm{S}}$ | $[\pm\langle 45\vert 15\rangle]_{2,\mathrm{S}}$ |
|---|---|---|---|---|---|
| 1 | 715.1<br>(714.8) | 782.1<br>(782.8) | 833.9<br>(835.3) | 858.6<br>(860.1) | 855.2<br>(856.2) |
| 2 | 1165.1<br>(1168.0) | 1223.2<br>(1224.0) | 1300.6<br>(1302.0) | 1382.8<br>(1385.0) | 1458.0<br>(1460.0) |
| 3 | 1858.8<br>(1873.0) | 1912.7<br>(1922.0) | 2019.7<br>(2026.0) | 2028.9<br>(2039.0) | 1933.0<br>(1940.0) |
| 4 | 1928.2<br>(1933.0) | 2025.7<br>(2034.0) | 2061.4<br>(2072.0) | 2169.1<br>(2175.0) | 2330.9<br>(2336.0) |
| Mode No. | $[\pm\langle 45\vert 30\rangle]_{2,\mathrm{S}}$ | $[\pm\langle 45\vert 45\rangle]_{2,\mathrm{S}}$ | $[\pm\langle 45\vert 60\rangle]_{2,\mathrm{S}}$ | $[\pm\langle 45\vert 75\rangle]_{2,\mathrm{S}}$ | $[\pm\langle 45\vert 90\rangle]_{2,\mathrm{S}}$ |
| 1 | 830.0<br>(830.5) | 793.8<br>(793.9) | 759.3<br>(759.2) | 738.2<br>(738.1) | 731.4<br>(731.6) |
| 2 | 1516.9<br>(1518.0) | 1521.9<br>(1523.0) | 1395.4<br>(1395.0) | 1271.4<br>(1272.0) | 1198.2<br>(1201.0) |
| 3 | 1791.6<br>(1795.0) | 1664.6<br>(1665.0) | 1666.3<br>(1667.0) | 1709.7<br>(1710.0) | 1761.9<br>(1762.0) |
| 4 | 2437.3<br>(2441.0) | 2426.7<br>(2429.0) | 2288.8<br>(2290.0) | 2049.8<br>(2058.0) | 1888.4<br>(1913.0) |

# 2 Parametric Studies on Buckling and Free Vibration of Unstiffened and Stiffened Laminated Plate (Section V. C)

## 2.1 Parametric Study on Free Vibration Responses (Section V. C. 1)

Figures 2 shows the parametric study results of the free vibration fundamental frequency in terms of different fiber path at different boundary conditions.

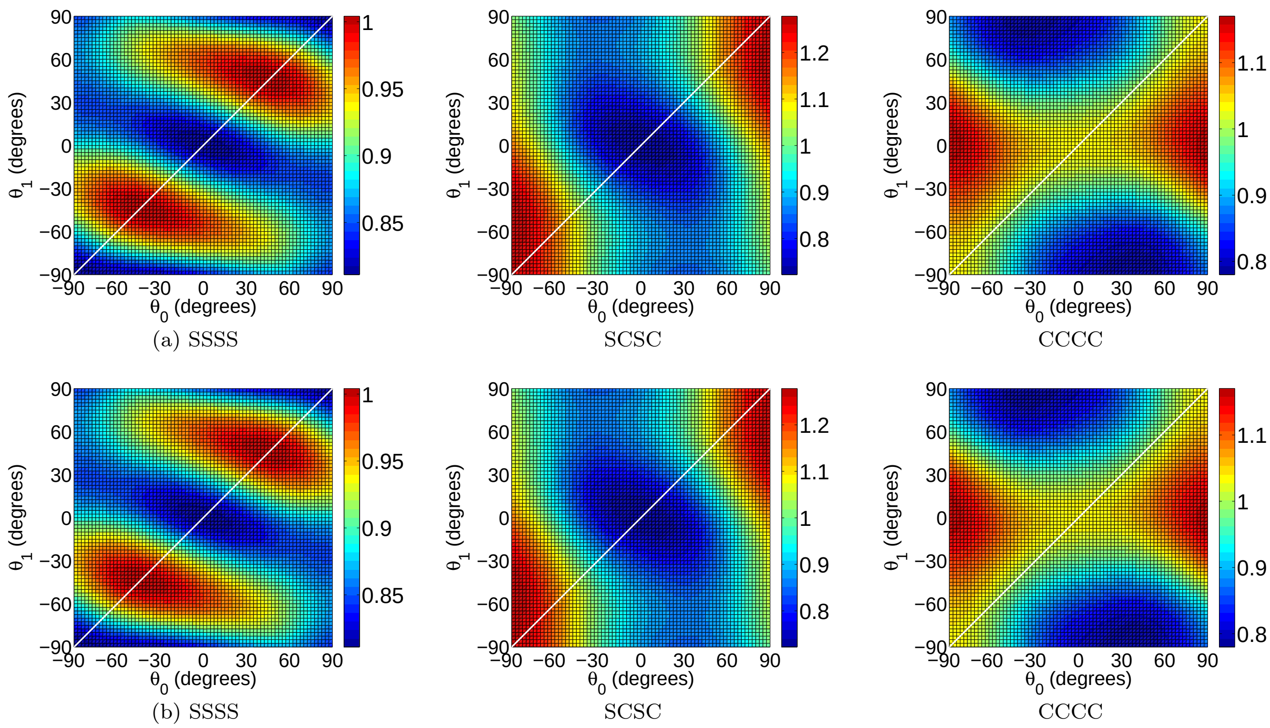


Figure 2: Normalized frequency $\omega_v/\omega_{v,QI}$ corresponding to the free vibration fundamental frequency for (a) unstiffened and (b) stiffened VAT laminated plate in terms of fiber ply orientations

## 2.2 Parametric Study on Buckling Loads (Section V. C. 2)

Figure 3 shows the parametric study results of the critical buckling load in terms of different fiber path for the plate at different boundary conditions.

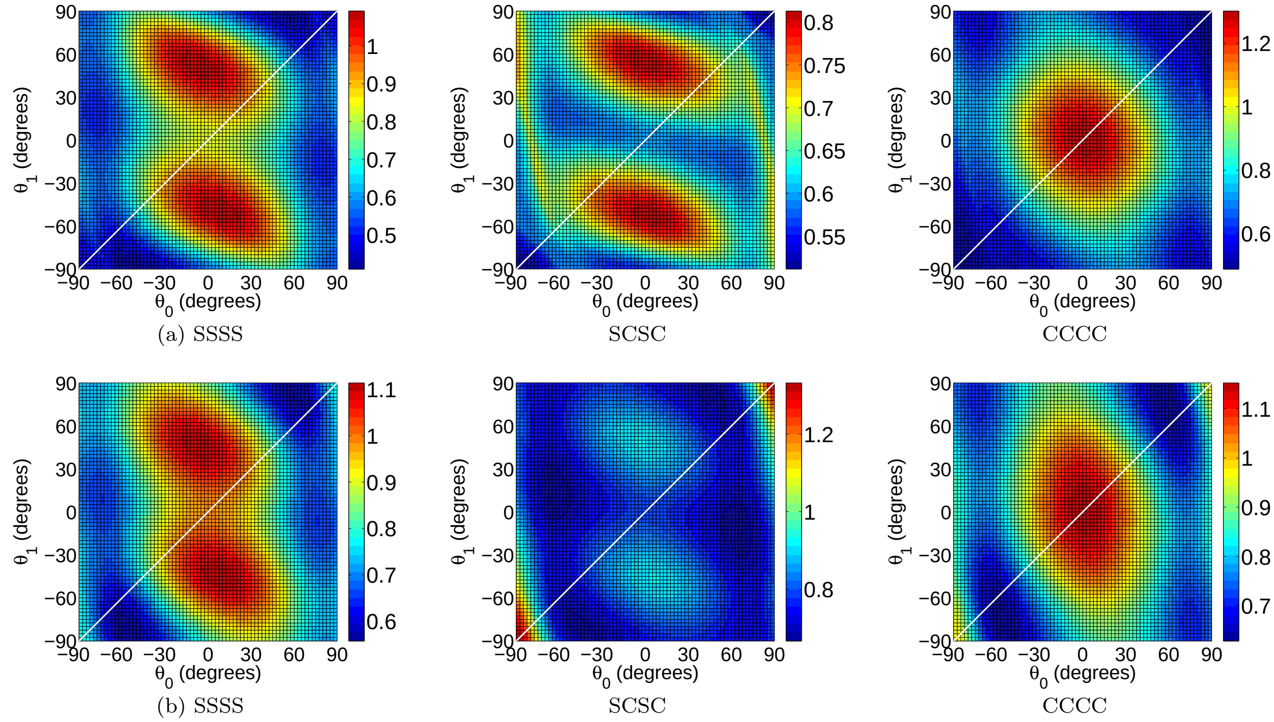


Figure 3: Normalized buckling load, $P_{cr}/P_{cr,QI}$ for (a) unstiffened and (b) stiffened VAT laminated plate in terms of fiber ply orientations

## 2.3 Maximum normalized eigenvalue of the prestressed vibration for unstiffened VAT plate from a parametric study (Section V. D)

Figure 4 shows both straight fiber paths and LV fiber paths for the maximum prestressed vibration eigenvalue at three representative load factors at three different boundary conditions.

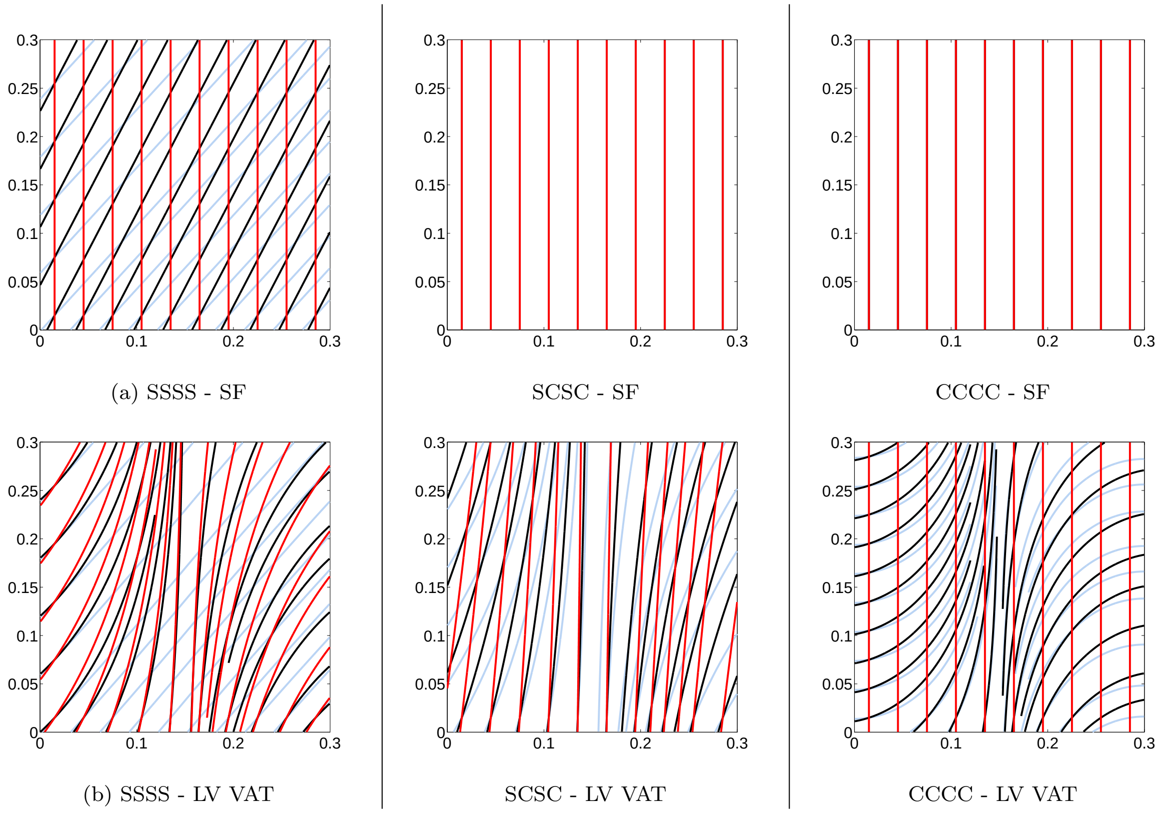


(a) SSSS - SF    SCSC - SF    CCCC - SF

(b) SSSS - LV VAT    SCSC - LV VAT    CCCC - LV VAT

Figure 4: Straight and LV fiber paths orientations for **unstiffened plates**, 10% $N_{cr,QI}$ ( ), 50% $N_{cr,QI}$ ( ) and 100% $N_{cr,QI}$ ( ), at three different boundary conditions, corresponding to the maximum eigenvalues in parametric studies

# 3 Verifications of Optimally NLV fiber path for Stiffened Laminated Plate on Free Vibration Results (Section VI. A)

## 3.1 Boundary Condition: SSSS

The optimal fiber path angles, $\theta_{mn}$, at reference points are:

$$\Theta_1 : \theta_{mn} = \begin{bmatrix} 48.36 & 47.40 & 43.38 \\ 43.60 & 44.65 & 46.29 \\ 55.22 & 46.06 & 44.25 \end{bmatrix} \text{degrees}$$

Table 2: Comparisons of mode frequency between present and NASTRAN results (Hz)

| Mode | NASTRAN | Present | Diff. |
|---|---|---|---|
| 1 | 90.7814 | 90.7016 | -0.0879% |
| 2 | 173.1056 | 173.0971 | -0.0049% |
| 3 | 271.0852 | 269.7848 | -0.4797% |
| 4 | 316.0163 | 315.9565 | -0.0189% |

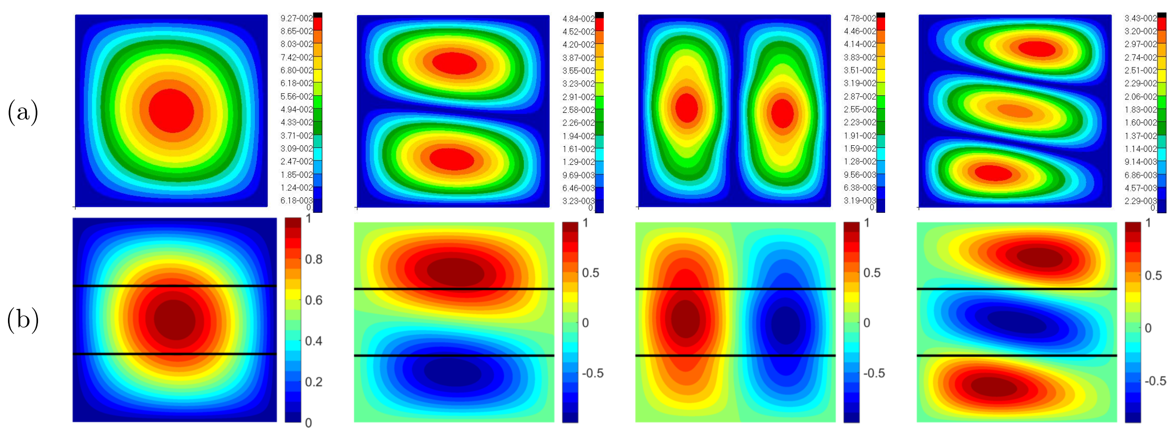


Figure 5: Free vibration mode shapes between the present and NASTRAN results: (a) NASTRAN results and (b) present results

### 3.2 Boundary Condition: SCSC

The optimal fiber path angles, $\theta_{mn}$, at reference points are:

$$\Theta_1 : \theta_{mn} = \begin{bmatrix} 90.00 & 90.00 & 65.37 \\ 90.00 & 60.55 & 37.70 \\ 90.00 & 90.00 & 65.04 \end{bmatrix} \text{degrees}$$

Table 3: Comparisons of mode frequency between present and NASTRAN results (Hz)

| Mode | NASTRAN | Present | Diff. |
|---|---|---|---|
| 1 | 135.4672 | 135.3706 | -0.0713% |
| 2 | 269.5315 | 267.7994 | -0.6426% |
| 3 | 313.5504 | 313.4713 | -0.0252% |
| 4 | 420.2409 | 418.7317 | -0.3591% |

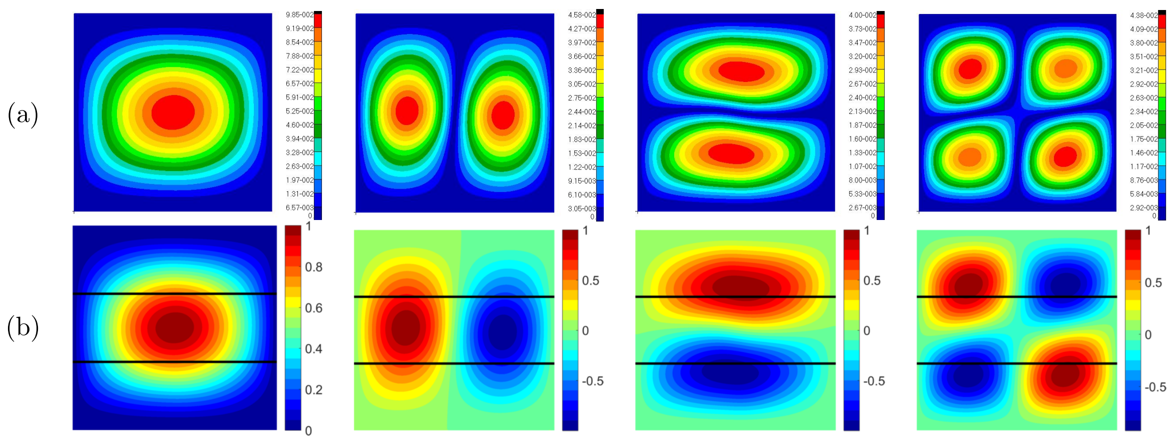


Figure 6: Free vibration mode shapes between the present and NASTRAN results: (a) NASTRAN results and (b) present results

## 3.3 Boundary Condition: CCCC

The optimal fiber path angles, $\theta_{mn}$, at reference points are:

$$\Theta_1 : \theta_{mn} = \begin{bmatrix} 86.41 & 56.45 & -16.72 \\ 64.35 & 45.62 & -0.15 \\ 90.00 & 90.00 & 15.88 \end{bmatrix} \text{degrees}$$

Table 4: Comparisons of mode frequency between present and NASTRAN results (Hz)

| Mode | NASTRAN | Present | Diff. |
|---|---|---|---|
| 1 | 193.0149 | 192.1570 | -0.4584% |
| 2 | 333.1762 | 332.3312 | -0.2536% |
| 3 | 406.3418 | 401.8433 | -1.1071% |
| 4 | 536.1451 | 531.0967 | -0.9416% |

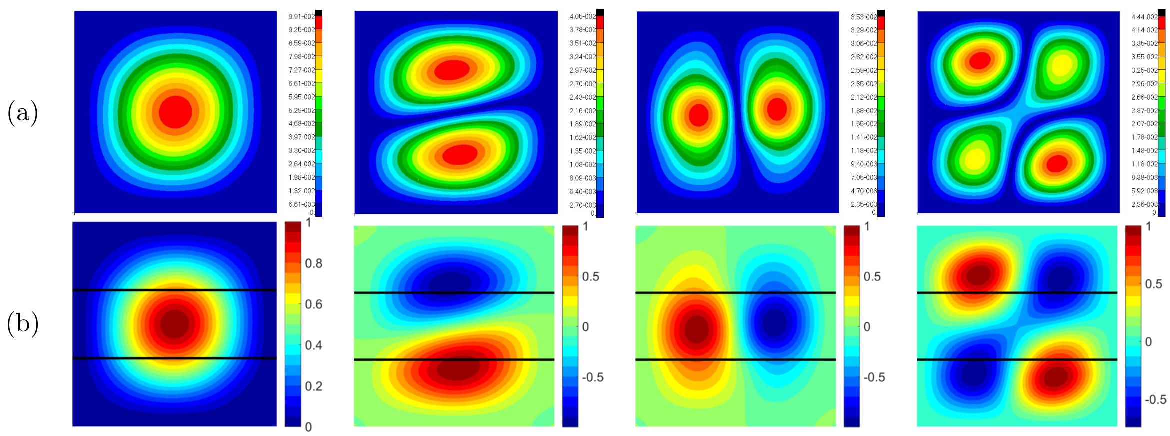


Figure 7: Free vibration mode shapes between the present and NASTRAN results: (a) NASTRAN results and (b) present results

# 4 Verifications of Optimally NLV fiber path for Stiffened Laminated Plate on Buckling Results (Section VI. A)

## 4.1 Boundary Condition: SSSS

The optimal fiber path angles, $\theta_{mn}$, at reference points are:

$$\Theta_1 : \theta_{mn} = \begin{bmatrix} 90.00 & 90.00 & 51.80 \\ -24.40 & 83.58 & 70.92 \\ 13.92 & -20.84 & -23.27 \end{bmatrix} \text{degrees}$$

Table 5: Comparisons of buckling eigenvalues between the present and NASTRAN results

| Mode | NASTRAN | Present | Diff. |
|---|---|---|---|
| 1 | 1.6099 | 1.6065 | -0.2126% |
| 2 | 2.2459 | 2.2459 | -0.0013% |
| 3 | 2.6831 | 2.6739 | -0.3448% |
| 4 | 2.8011 | 2.7922 | -0.3188% |

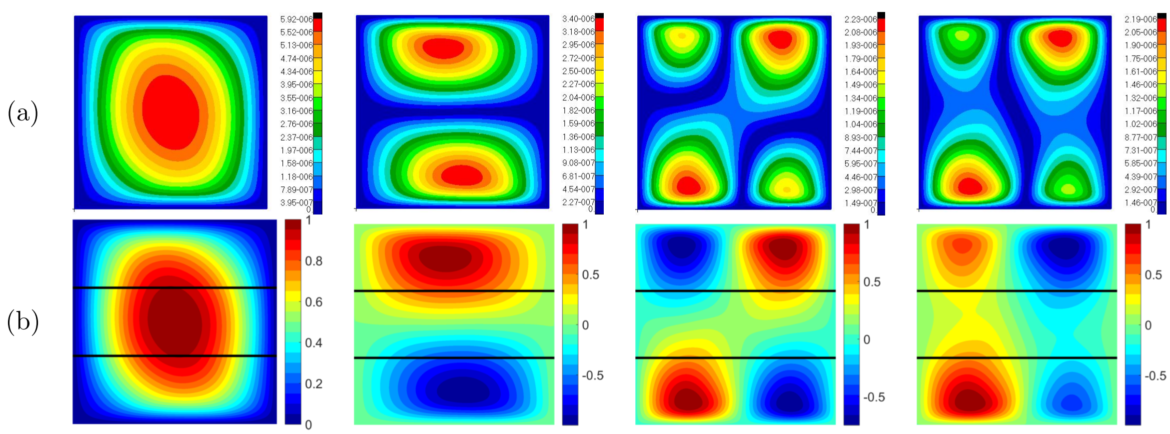


Figure 8: Comparisons of the first four buckling mode shapes between (a) NASTRAN results and (b) present results

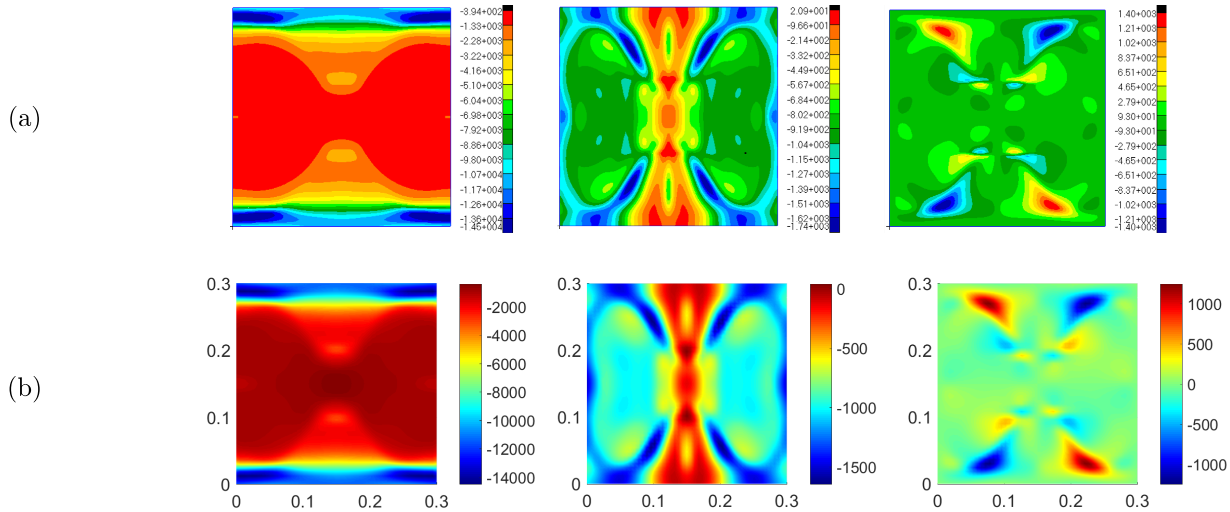


Figure 9: Comparisons of in-plane stress resultants, $N_{xx}$, $N_{yy}$ and $N_{xy}$, between (a) NASTRAN results and (b) present results

## 4.2 Boundary Condition: SCSC

The optimal fiber path angles, $\theta_{mn}$, at reference points are:

$$\Theta_1 : \theta_{mn} = \begin{bmatrix} 90.00 & 90.00 & 79.21 \\ 45.18 & 57.57 & 46.66 \\ -90.00 & -90.00 & 38.29 \end{bmatrix} \text{degrees}$$

Table 6: Comparisons of buckling eigenvalues between the present and NASTRAN results

| Mode | NASTRAN | Present | Diff. |
|---|---|---|---|
| 1 | 2.7239 | 2.7011 | -0.8335% |
| 2 | 4.1160 | 4.7056 | -0.9813% |
| 3 | 4.2535 | 4.2080 | -1.0676% |
| 4 | 4.2629 | 4.2148 | -1.1291% |

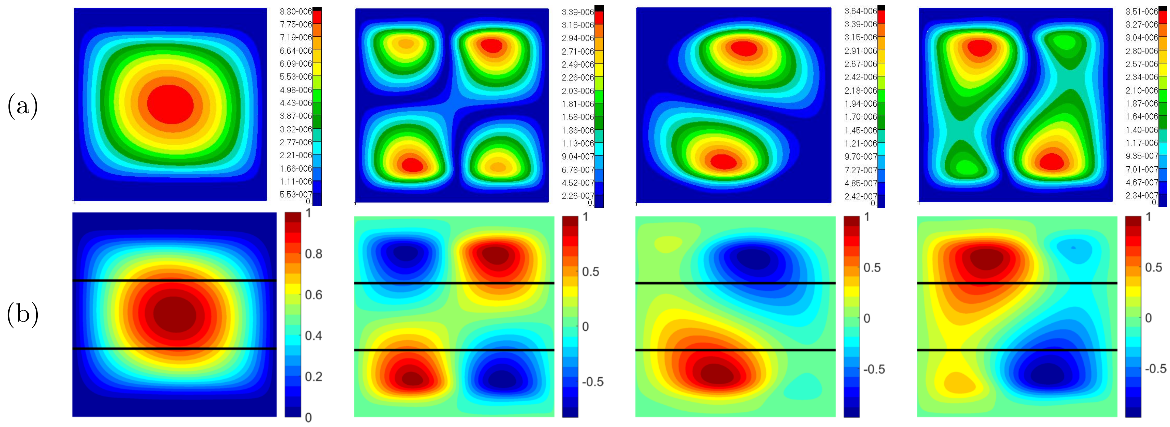


Figure 10: Comparisons of the first four buckling mode shapes between (a) NASTRAN results and (b) present results

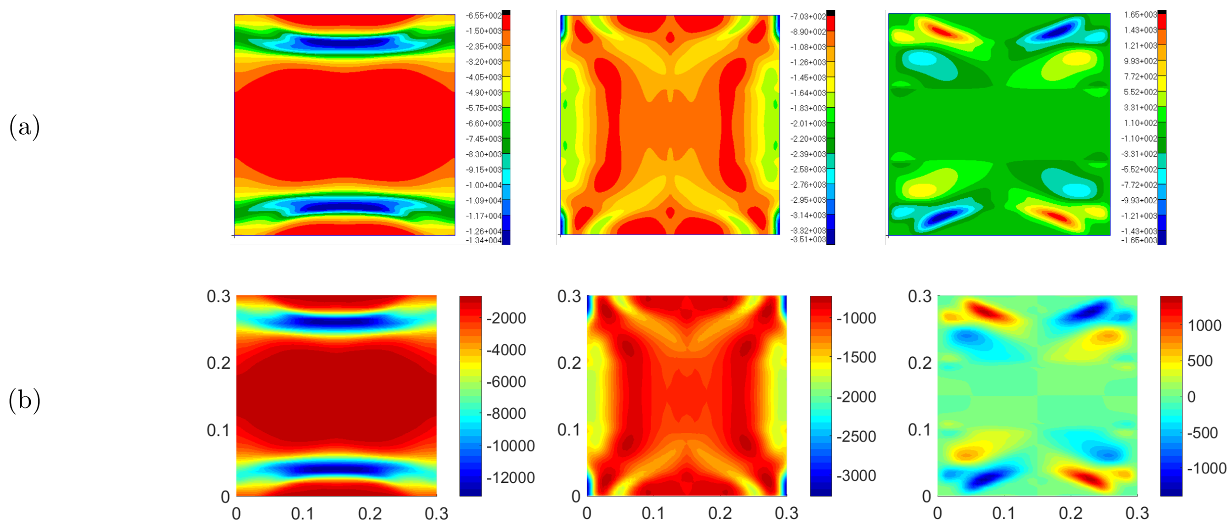


Figure 11: Comparisons of in-plane stress resultants, $N_{xx}$, $N_{yy}$ and $N_{xy}$, between the present and NASTRAN results: (a) NASTRAN results and (b) present results

## 4.3 Boundary Condition: CCCC

The optimal fiber path angles, $\theta_{mn}$, at reference points are:

$$\Theta_1 : \theta_{mn} = \begin{bmatrix} 90.00 & 76.26 & -12.24 \\ -20.83 & 90.00 & -36.86 \\ 9.89 & -19.81 & 11.41 \end{bmatrix} \text{degrees}$$

Table 7: Comparisons of buckling eigenvalues between the present and NASTRAN results

| Mode | NASTRAN | Present | Diff. |
|---|---|---|---|
| 1 | 4.9991 | 4.9461 | -1.0590% |
| 2 | 5.1417 | 5.1123 | -0.5718% |
| 3 | 5.5705 | 5.4984 | -1.2930% |
| 4 | 5.6432 | 5.5854 | -1.0245% |

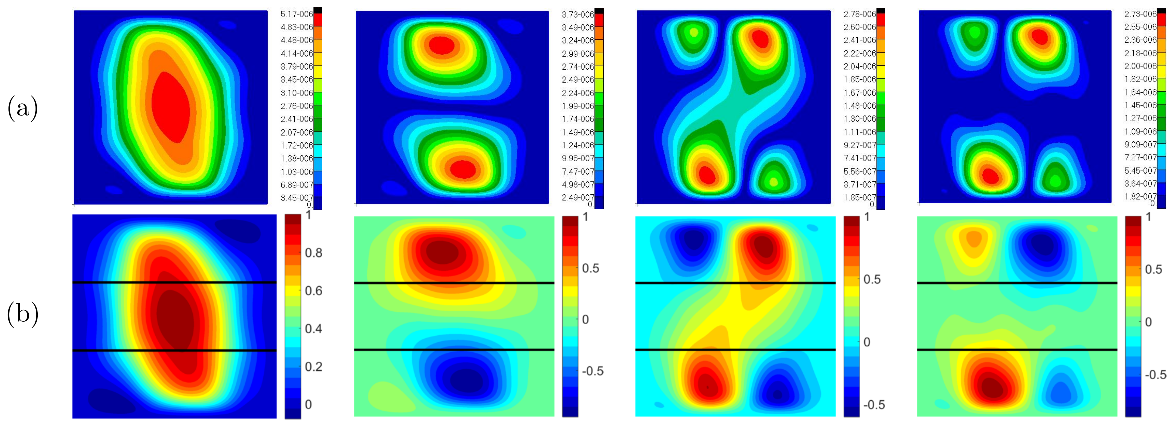


Figure 12: Comparisons of the first four buckling mode shapes between (a) NASTRAN results and (b) present results

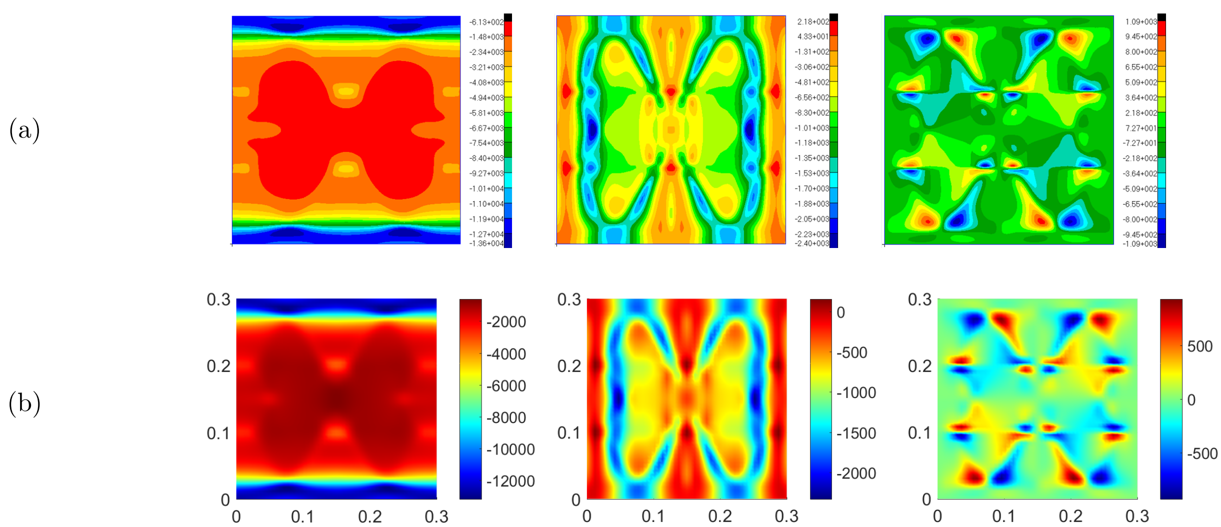


Figure 13: Comparisons of in-plane stress resultants, $N_{xx}$, $N_{yy}$ and $N_{xy}$, between (a) NASTRAN results and (b) present results

# 5 Optimal NLV Fiber Paths for Maximum Prestressed Vibration Fundamental Frequency

## 5.1 Boundary Condition: SSSS

The optimal fiber path angles, $\theta_{mn}$, at reference points are:

$$w_0 = 10\% \qquad \Theta_1 : \theta_{mn} = \begin{bmatrix} 90.00 & 89.67 & 46.35 \\ 90.00 & 53.95 & 48.68 \\ 90.00 & 45.86 & 51.69 \end{bmatrix} \text{degrees}$$

$$w_0 = 50\% \qquad \Theta_1 : \theta_{mn} = \begin{bmatrix} 90.00 & 90.00 & 86.87 \\ 90.00 & 72.52 & 39.80 \\ 90.00 & 56.13 & 44.37 \end{bmatrix} \text{degrees}$$

$$w_0 = 100\% \qquad \Theta_1 : \theta_{mn} = \begin{bmatrix} 87.98 & 89.78 & 90.00 \\ 87.06 & 90.00 & 39.36 \\ 90.00 & 69.16 & 31.70 \end{bmatrix} \text{degrees}$$

## 5.2 Boundary Condition: SCSC

The optimal fiber path angles, $\theta_{mn}$, at reference points are:

$$w_0 = 10\% \qquad \Theta_1 : \theta_{mn} = \begin{bmatrix} 90.00 & 90.00 & 76.01 \\ 90.00 & 65.39 & 34.61 \\ 90.00 & 90.00 & 70.38 \end{bmatrix} \text{degrees}$$

$$w_0 = 50\% \qquad \Theta_1 : \theta_{mn} = \begin{bmatrix} 90.00 & 90.00 & 90.00 \\ 90.00 & 77.55 & 31.00 \\ 88.72 & 90.00 & 78.54 \end{bmatrix} \text{degrees}$$

$$w_0 = 100\% \qquad \Theta_1 : \theta_{mn} = \begin{bmatrix} 89.30 & 90.00 & 76.01 \\ 89.69 & 82.50 & 35.34 \\ 87.71 & 90.00 & 77.80 \end{bmatrix} \text{degrees}$$

### 5.3 Boundary Condition: CCCC

The optimal fiber path angles, $\theta_{mn}$, at reference points are:

$$w_0 = 10\% \qquad \Theta_1 : \theta_{mn} = \begin{bmatrix} 90.00 & 66.36 & -17.35 \\ 90.00 & 50.20 & 44.65 \\ 90.00 & 90.00 & 46.78 \end{bmatrix} \text{degrees}$$

$$w_0 = 50\% \qquad \Theta_1 : \theta_{mn} = \begin{bmatrix} 90.00 & 76.62 & -16.92 \\ 89.92 & 68.58 & -9.05 \\ 87.93 & 90.00 & 65.20 \end{bmatrix} \text{degrees}$$

$$w_0 = 100\% \qquad \Theta_1 : \theta_{mn} = \begin{bmatrix} 83.66 & 80.32 & -19.24 \\ 86.53 & 78.94 & -36.19 \\ 89.50 & 90.00 & 90.00 \end{bmatrix} \text{degrees}$$

## References

[1] Rodrigues, J. D., Ribeiro, P., and Akhavan, H., “Experimental and Finite Element Modal Analysis of Variable Stiffness Composite Laminated Plates,” *11th International Conference on Vibration Problems (ICOVP-2013)*, Lisbon, Portugal, 2013.

[2] Ribeiro, P. and Akhavan, H., “Non-linear Vibrations of Variable Stiffness Composite Laminated Plates,” *Composite Structures*, Vol. 94, No. 8, 2012, pp. 2424–2432.